

Plasma diagnostics for the control of reactive magnetron deposition process

F. Perry ^a, B. Stauder ^b, G. Henrion ^{a*}, Ph. Pigeat ^b

^a *Laboratoire de Physique des Milieux Ionisés (CNRS URA 835), B.P. 239, F 54506 Vandoeuvre lès Nancy Cedex, France*

^b *Laboratoire de Sciences et Génie des Surfaces (CNRS URA 1402), Ecole des Mines, Parc de Saurupt, F 54042 Nancy Cedex, France*

Abstract

Many plasma diagnostic methods are usually studied in laboratories in order to understand the fundamental processes that govern the plasma. This paper aims to study the potentialities of such diagnostics performed in a specific magnetron industrial-type deposition reactor in which the form of the time variation of the electrical plasma parameters ($U(t)$; $I(t)$) depends on the mean power applied to the electrodes. In particular, Langmuir probe and optical emission spectroscopy (OES) measurements are carried out in the case of aluminium nitride and oxide deposition. Ex-situ coating analysis is performed by means of optical microscopy, scanning electron microscopy, microprobe analysis and Auger spectroscopy. In this paper we show that the Langmuir probe is not a well-adapted diagnostic method to study such reactive plasmas. Indeed, the high deposition rate implies a fast modification of the probe geometry and electrical properties due to the deposition of a thin film on the probe tip. On the other hand, OES measurements are related to the stoichiometry of the deposited coatings. Some phenomenological interrelations between the mean lines intensity and the coating stoichiometry are found, which may be used to control the deposition process.

Keywords: Emission spectroscopy; Magnetron; Al_2O_3 deposition; Process control; Coating stoichiometry

1. Introduction

It has been apparent for many years that the understanding of surface phenomena as well as the optimization and the control of plasma-assisted surface treatments need a detailed characterization of the plasma (see, for instance, Ref. [1]). Indeed, it is necessary to be able to relate the physico-chemical properties of the layer (composition, stoichiometry and crystallographic structure) to the deposition conditions: that is, to the parameters and the different species that govern the plasma. For this, mass spectrometry [2,3], Langmuir probe [4,5] and optical emission spectroscopy (OES) [6–8] are the most frequently used plasma diagnostic methods. In our study of a specific industrial-type deposition reactor, we have chosen to carry out plasma diagnostics by means of electrostatic probes and OES. These diagnostic methods are commonly used in our laboratory to describe and understand the specific phenomena occurring in various plasmas. For this work, they are used to find some phenomenological interrelations between the plasma characteristics and the properties of

the deposited layers, independently of the change in the shape of the discharge voltage and current with the mean applied power. In this paper, the experimental set-up is described first. Then the distortion of the probe characteristic which is due to the probe tip contamination is briefly discussed. Finally, OES results that concern the deposition of Al_2O_3 and AlN are reported.

2. Experimental details

A schematic drawing of our specific industrial-type plasma reactor is shown in Fig. 1. It consists of a cylindrical stainless steel vessel 40 cm in diameter, 40 cm high, with 50 l usable volume. A diffusion pump makes possible a residual pressure of about 10^{-4} Pa. The pumping speed is 130 l s^{-1} at our running pressure condition. The gas inlet is controlled by means of mass flowmeters, and an absolute pressure gauge is used to control the pressure. The target (50 mm diameter) placed on the magnetron is biased to a rectified negative voltage. The particular shape of the discharge voltage and current are given for different mean powers in Fig. 2. The substrate holder is located 70 mm from the target.

* Corresponding author.

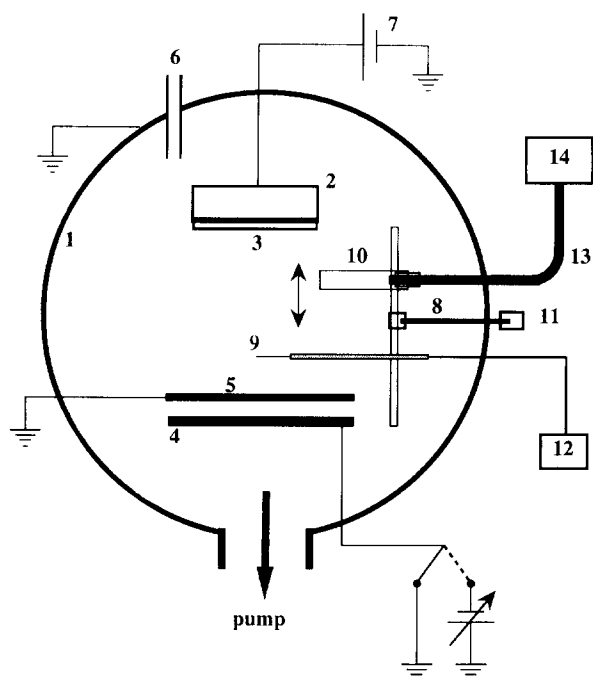


Fig. 1. Schematic drawing of the plasma reactor: 1, vacuum chamber; 2, magnetron; 3, target; 4, substrate holder; 5, protective shield; 6, gas inlet; 7, power supply; 8, probe and fibre-optic movable holder; 9, Langmuir probe; 10, fibre collimator; 11, stepping motor; 12, Langmuir probe data acquisition; 13, fibre bundle; 14, spectrometry data acquisition.

Though the substrate may be biased with a positive or negative voltage, the present work has been carried out with grounded substrate. The usual running conditions are as follows: constant discharge power 240 W, which corresponds to a mean current of 0.6 A and a mean voltage of 400 V in pure argon; total pressure 0.9 Pa; gas mixture Ar/O₂ or Ar/N₂.

The Langmuir probe, as well as a fibre optic, are fixed on a mechanical manipulator, thus allowing plasma diagnostics all over the target–substrate space.

The probe tip consists of a tungsten wire (0.2 mm diameter, 10 mm length) inserted in a stainless steel tube (0.2 mm i.d.), allowing easy replacement of the probe tip. Both are placed inside an insulating alumina pipe. A second alumina pipe (2 mm i.d.) is used to avoid electrical contact between probe tip and alumina, should the probe be coated with an aluminium layer (Fig. 3). Taking into account the periodical variation of the discharge voltage with time, the current–voltage probe characteristics have to be synchronized with the current alternations. For this we use a device similar to that described in detail by Bougdira et al. [9] and by Henrion et al. [5], in which we have replaced the programmable clock by a home-made 50 Hz pulse generator to achieve the desired synchronization of our measures with the power supply.

The light emitted by the plasma is detected by means of a home-made fibre-optic bundle consisting of 800

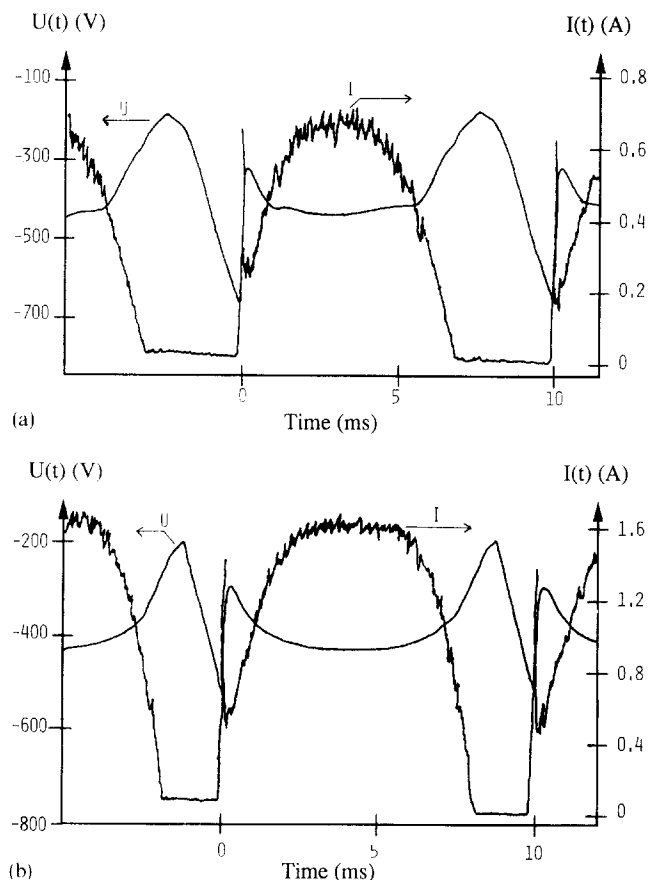


Fig. 2. Discharge voltage $U(t)$ and current $I(t)$ for different applied mean power P : (a) $P = 150$ W; (b) $P = 330$ W.

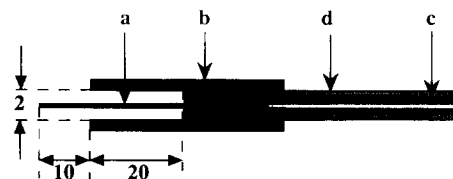


Fig. 3. Langmuir probe design: (a) tungsten probe tip; (b) alumina pipe; (c) stainless steel tube; (d) alumina pipe.

Si/SiO₂ single fibres (0.05 mm core diameter) maintained in a quartz wrapping for thermal and mechanical protection. At each end of the bundle, the single fibres are arranged in front of a rectangular slit (6 mm length; 0.5 mm width). A graphite collimator is placed around the optical end immersed in the plasma to avoid the optical surface being coated. Such a fibre optic allows a spatial resolution of 5 mm at a distance of 100 mm. The second fibre end is connected to a monochromator (Jobin Yvon HR 640; focal length 640 mm) equipped with a 1200 lines mm⁻¹ holographic grating. The optical signal can be measured either by a photomultiplier tube (Hamamatsu R636) over the wavelength range from 185 nm to 930 nm or by an intensified photodiode array (IRY 1024G/B) over the range from 200 nm to 800 nm. The photomultiplier output signal is recorded by a chart

recorder. The photodiode array is driven by PC software (Jobin Yvon Spectramax™) and thus runs as a multi-channel analyser.

3. Langmuir probes

Though it is limited to the measurement of electrons with relatively low energy (typically less than 10 eV), the single Langmuir probe is however a good tool to obtain a significant value of the electron mean energy and density, which may be correlated to the intensity of some emission lines of the plasma [10]. Nevertheless, the use of electrostatic probes for plasma diagnostics needs some care (generally one assumes that the probe does not disturb the plasma and that the probe potential is not affected by the probe current). The probe tip diameter and surface as well as the probe tip material are important parameters. Now in a reactive deposition plasma the probe is subjected to the same modifications as the treated substrates. This generally implies a noteworthy variation in the measured results [11–18]. To perform reliable and reproducible measurements it is necessary to control or to know permanently the surface state of the probe tip. Different procedures aiming to protect and/or clean the probe surface prior to each measurement has been proposed [19–23]. Some authors have reduced the exposure time of the probe to the plasma by very fast data acquisition [14,18,24,25]. This technique, which is well adapted to d.c. plasma, cannot be applied to characterize the plasma during the fast rise and fall times in pulsed discharges (a sampling frequency of 250 MHz would be necessary to obtain a time resolution of 1 μ s for a probe characteristic digitized over 256 points). Moreover, the cleaning of the probe tip is necessary between successive probe characteristic acquisitions.

In this study we have tried to carry out probe measurements with different cleaning procedures (electronic bombardment [19–23], ionic bombardment [14–16]). Unfortunately, none of these methods allowed us to obtain reliable and reproducible results. Indeed, the deposition rate of aluminium on the probe tip (≈ 0.15 – $0.30 \mu\text{m min}^{-1}$) is too high and the probe tip is coated during the measure (≈ 5 s) with a 12.5–25 nm thick aluminium layer that distorts the results. Consequently, in our reactor, this diagnostic method cannot be used as an effective tool that could give some insights into the electron processes that occur in the plasma and influence the plasma reactivity. In order to overcome this problem, we are developing a new probe device that will allow us to renew the probe tip in situ and during the data acquisition.

4. Optical emission spectroscopy

The different optical transitions we have observed in this study are summarized in Table 1 with the corresponding wavelength in nanometres. The results reported hereafter deal with the influence of reactive gas flow rate on the coating stoichiometry and on the emission lines intensity for the systems Al/O₂, Al/N₂ and Fe–Cr–Ni/O₂.

4.1. Case of Al/O₂

The aluminium transition used corresponds to a resonant line to the ground state and can be considered as representative of the aluminium atoms density in the plasma [26] and thus of the metal atoms sputtered from the target. This assumption has been verified by measuring the aluminium line intensity correlated with the coating chemical composition, the weight loss of the target and the weight gain of the substrate [27]. The variation of the Al line as well as that of the AlO line as a function of the flow rate $d(\text{O}_2)$ of the reactive gas introduced into the reactor is reported in Fig. 4. The AlO line exhibits a clear maximum for $d(\text{O}_2)$ about 7.5 sccm while the Al line decreases as $d(\text{O}_2)$ increases (this decrease is characteristic of the target oxidation). This behaviour is directly linked to the target oxidation. The AlO molecules present in the vapour phase are

Table 1
Observed transitions and corresponding wavelengths

Element	Transition	Wavelength (nm)
Al	$4s^2S \rightarrow 3p^2P^0$	396.1
Fe	$z^5F^0 \rightarrow a^5D$	372.0
Cr	$y^7P^0 \rightarrow a^5S$	357.9
Ni	$z^3P \rightarrow a^3D$	352.4
AlO	$B^2\Sigma^+, v=0 \rightarrow X^2\Sigma^+, v=0$	484.2

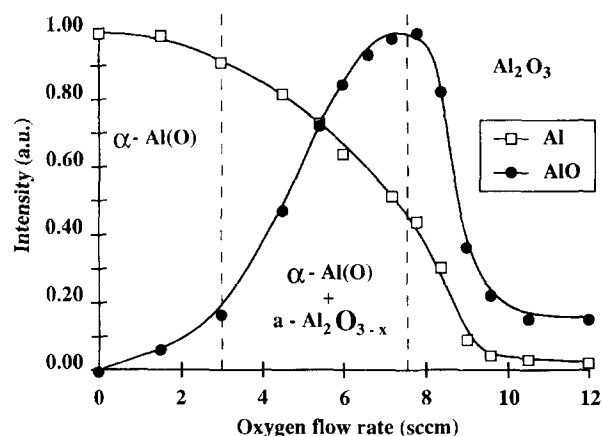


Fig. 4. Al and AlO lines intensity and coating composition as a function of $d(\text{O}_2)$. Intensities are normalized to 1 at the maximum value.

mostly ejected from the partially oxidized target. Indeed, the mean free path of the neutral species is high (≈ 2 cm according to the relation given by Pointu [28]), and the probability of forming AlO molecules in the gas phase is low.

The variation of the AIO line may thus be explained as follows. For low oxygen flow rate the sputtering rate is high and the quantity of sputtered AlO increases as the $d(\text{O}_2)$ increases: that is, as the target oxidizes. For higher $d(\text{O}_2)$ the sputtering rate decreases and the increase in target oxidation does not compensate this variation. We observe then a decrease in AIO line intensity. On the other hand, we have mentioned in Fig. 4 the composition of the deposited layer to be compared with the variation of the AIO line intensity as a function of $d(\text{O}_2)$. When the AIO line is increasing (i.e. for low $d(\text{O}_2)$) the layer is either α -Al(O) for flow rate less than 3 sccm or α -AlO + amorphous $\text{Al}_2\text{O}_{3-x}$. The perfect stoichiometry of amorphous alumina is reached for $d(\text{O}_2)$ greater than or equal to that corresponding to the maximum of AIO emission line intensity ($d(\text{O}_2) \approx 7.5$ sccm). It is thus possible to ensure the right stoichiometry of the deposited Al_2O_3 by using the optical signal of AIO to control the oxygen flow rate.

4.2. Case of Al/N

As for the previous case the variation of the Al line as a function of the nitrogen flow rate $d(\text{N}_2)$ is significant for the target nitriding. Indeed, the decrease of the Al line intensity as $d(\text{N}_2)$ increases is quite linear for low $d(\text{N}_2)$, i.e. as the target is being progressively nitrided (Fig. 5). When the target is totally nitrided, the Al line intensity keeps a constant value as $d(\text{N}_2)$ increases. In Fig. 5 is also reported the concentration of nitrogen atoms in the coating as well as its composition. As for Al/ O_2 we observe that the AlN stoichiometry of the coating is reached only for a complete nitriding of the target ($d(\text{N}_2) \approx 8.5$ sccm). Before this the layer is either

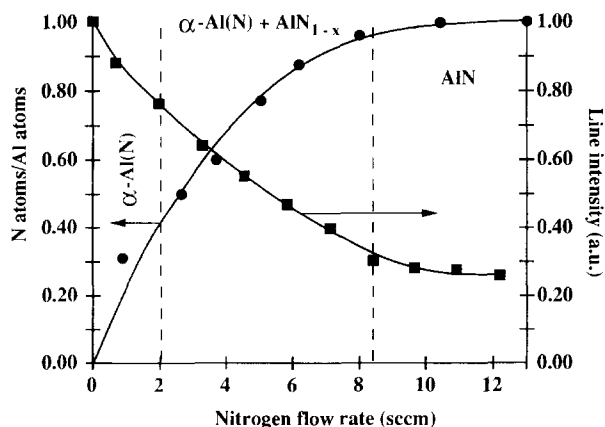


Fig. 5. Al line intensity and coating composition as a function of $d(\text{N}_2)$. Intensities are normalized to 1 at the maximum value.

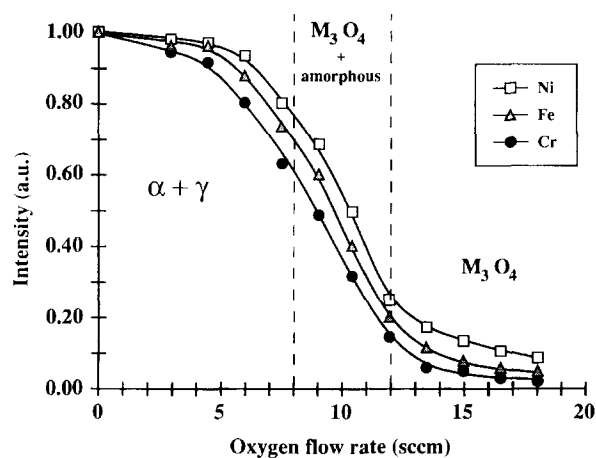


Fig. 6. Fe, Cr and Ni lines intensity and coating composition as a function of $d(\text{O}_2)$. Intensities are normalized to 1 at the maximum value. For $d(\text{O}_2)=0$, the lines intensity ratios are as follows: $I(\text{Cr})/I(\text{Ni})=10$; $I(\text{Cr})/I(\text{Fe})=2.5$.

α -Al(N) or under-stoichiometric AlN_{1-x} . From these results it appears that it is possible to control the stoichiometry of the deposited AlN compound by a direct measurement of the Al line intensity.

4.3. Other case

Similar results, which lead to the possible control of the coating stoichiometry by means of emission spectroscopy, have been obtained in the case of Fe–Cr–Ni/ O_2 . As for AlN and Al_2O_3 , stoichiometric oxide M_3O_4 ($\text{M} = \text{Fe, Cr, Ni}$) is elaborated for a complete target oxidation (Fig. 6). Nevertheless, in this case, the highest intensity of the chromium line compared with those of iron and nickel is more suitable for the control of the process.

5. Conclusion

In a specific industrial-type deposition reactor in which the shape of the discharge voltage and current ($U(t)$; $I(t)$) varies with the applied mean power, OES results have been obtained by simply measuring the mean value of the lines intensity. There are no studies in the literature that describe or take into account these variations of $U(t)$ and $I(t)$. Moreover, the existence of simple relations between the characteristics of a coating (that is in fact a mean result) and the measurement of mean value of plasma parameters was a priori not obvious.

The presented results show that such phenomenological interrelations exist and are significant, even with a power supply that is not well stabilized. In the particular cases of the systems Al/ O_2 , Al/ N_2 and stainless steel/ O_2 , the direct correlation that has been found between the lines intensity and the coating stoichiometry may be

useful to control the process by adjusting the gas flow rate to obtain the desired layer composition.

References

- [1] *Proc. 3rd Int. Conf. Plasma Surface Engineering, Garmisch-Partenkirchen, 1992, Surf. Coat. Technol.*, 59–60 (1993).
- [2] A. Okamoto and T. Serikawa, *Thin Solid Films*, 137 (1986) 143.
- [3] S. Berg, H.O. Blohm, M. Moradi and C. Nender, *J. Vac. Sci. Technol.*, A7 (1989) 1225.
- [4] M. Boumerzoug, R.V. Kruzelecky, P. Mascher and D. Thompson, *Surf. Coat. Technol.*, 59 (1993) 77.
- [5] G. Henrion, M. Fabry, R. Hugon and J. Bougdira, *Plasma Sources Sci. Technol.*, 1 (1992) 117.
- [6] K. Salmenoja, A.S. Korhonen and M.S. Sulonen, *J. Vac. Sci. Technol.*, A3 (1985) 2364.
- [7] S. Schiller, U. Heisig, K. Steinfeld, J. Strümpfel, A. Friedrich and R. Fricke, in *Proc. 6th Int. Conf. on Ion and Plasma Assisted Technology (IPAT'87)*, Brighton, 1987, CEP Consultants, Edinburgh, p. 23.
- [8] A. Brundnik, H. Czternastek, K. Zakrzewska and M. Jachimowski, *Thin Solid Films*, 199 (1991) 45.
- [9] J. Bougdira, G. Henrion and M. Fabry, *J. Phys. D Appl. Phys.*, 24 (1991) 1076.
- [10] R. Hugon, G. Henrion and M. Fabry, *Surf. Coat. Technol.*, 59 (1993) 82.
- [11] G. Wehner and G. Medicus, *J. Appl. Phys.*, 23 (1952) 1035.
- [12] W.R. Larsen, C.W. Wilmsen and P.W. Chan, *J. Appl. Phys.*, 44 (1973) 2153.
- [13] K. Wieseman, Int. Rapport 87–05–164, Inst. Experim. Phys., AG II, Bochum, Germany, 1987, unpublished.
- [14] J.F. Waymouth, *J. Appl. Phys.*, 30 (1959) 1404.
- [15] P. Spatenka and M. Sicha, *Contrib. Plasma Phys.*, 29 (1989) 57.
- [16] R.A. Olson, *J. Appl. Phys.*, 43 (1972) 2785.
- [17] S. Yamaguchi, G. Sawa and M. Ieda, *Jpn. J. Appl. Phys.*, 21 (1982) L610.
- [18] E.P. Szuszczyewicz and J.C. Holmes, *J. Appl. Phys.*, 46 (1975) 5134.
- [19] A.G. Coulter and G.S. Higginson, *J. Elec. Control*, 15 (1963) 437.
- [20] P.A. Bagryanskii and E.V. Shun'ko, *Prib. Tekh. Eksperimenta*, 2 (1986) 166.
- [21] G. Lempriere and J.M. Poitevin, *Vacuum*, 37 (1987) 825.
- [22] B.C. Bell and D.A. Glocker, *J. Vac. Sci. Technol.*, A6 (1988) 2047.
- [23] M.A. Easley, *J. Appl. Phys.*, 22 (1951) 590.
- [24] K. Hirao and K. Oyuma, *Geomag. Geoelectr.*, 24 (1972) 415.
- [25] P. Spatenka, R. Studeny and H. Suhr, *Meas. Sci. Technol.*, 3 (1992) 704.
- [26] J. Affinito and R.R. Parson, *J. Vac. Sci. Technol.*, A2–3 (1984) 1275.
- [27] B. Stauder, *Ph.D. Thesis*, INPL, Nancy, 1994.
- [28] A.M. Pointu, in A.M. Pointu and A. Ricard (eds.), *Réactivité dans les Plasmas*, Les Éditions de Physique, Paris, 1984, pp. 1–57.